Neurotoxicology 75 (2019) 209–220

Contents lists available at ScienceDirect

Neurotoxicology

journal homepage: www.elsevier.com/locate/neuro

Full Length Article

Influence of selenium on the emergence of neuro tubule defects in a neuron-like cell line and its implications for amyotrophic lateral sclerosis

Tullia Maraldi[a,*,1], Francesca Beretti[a,1], Laura Anselmi[b], Cinzia Franchin[c,d], Giorgio Arrigoni[c,d], Luca Braglia[b], Jessica Mandrioli[e], Marco Vinceti[b,f], Sandra Marmiroli[b]

[a] Department of Surgical, Medical, Dental and Morphological Sciences with interest in Transplant, Oncology and Regenerative Medicine, University of Modena and Reggio Emilia, Via Del Pozzo 71, 41124, Modena, Italy
[b] Department of Biomedical, Metabolic and Neural Sciences, University of Modena and Reggio Emilia, Modena, 41125, Italy
[c] Department of Biomedical Sciences, University of Padova, via G. Basso 58/B, 35131, Padova, Italy
[d] Proteomics Center, University of Padova and Azienda Ospedaliera di Padova, via G. Orus 2/B, 35129, Padova, Italy
[e] Neurology Unit, Department of Neurosciences, Azienda Ospedaliero Universitaria di Modena, Modena, Italy
[f] Department of Epidemiology, Boston University School of Public Health, Boston, Massachusetts, United States

ARTICLE INFO

Keywords:
Selenium
ALS
Tubulin alpha-4A
Cytoskeleton
Neurodegeneration

ABSTRACT

Impairment of the axonal transport system mediated by intracellular microtubules (MTs) is known to be a major drawback in neurodegenerative processes.

Due to a growing interest on the neurotoxic effects of selenium in environmental health, our study aimed to assess the relationship between selenium and MTs perturbation, that may favour disease onset over a genetic predisposition to amyotrophic lateral sclerosis.

We treated a neuron-like cell line with sodium selenite, sodium selenate and seleno-methionine and observed that the whole cytoskeleton was affected. We then investigated the protein interactome of cells overexpressing αTubulin-4A (TUBA4A) and found that selenium increases the interaction of TUBA4A with DNA- and RNA-binding proteins. TUBA4A ubiquitination and glutathionylation were also observed, possibly due to a selenium-dependent increase of ROS, leading to perturbation and degradation of MTs. Remarkably, the TUBA4A mutants R320C and A383 T, previously described in ALS patients, showed the same post-translational modifications to a similar extent. In conclusion this study gives insights into a specific mechanism characterizing selenium neurotoxicity.

1. Introduction

Amyotrophic lateral sclerosis (ALS) is an aggressive multifactorial disease characterized by the degeneration of motor neurons (MNs), their axons and neuromuscular synapses. The vulnerability of MNs may depend on a wide range of complex factors, among which a dysfunction of neuronal microtubules (MTs) that are intracellular structures that allow many neuronal functions, including axonal transport. In ALS, MTs abnormalities have been suggested to be a key component of the disease, at least in some cases(Clark et al., 2016). Indeed, the recent identification of microtubule protein mutations and their impact on MT function, specific interactions with mutant and pathological proteins as well as altered function of MT-associated proteins and signaling pathways which affect MT dynamics, have all been implicated in ALS etiopathogenesis (Smith et al., 2014)(Tischfield et al., 2011). Not only in the vast majority of sporadic cases are present disruptions in this intracellular machinery, but mutation of a microtubule protein, the tubulin isoform TUBA4A, may also cause a familial, albeit rare, form of

Abbreviations: BSA, Bovine serum albumin; DCFH-DA, dichlorodihydrofluorescein diacetate; DABCO, 1,4-diazabicyclo(2.2.2)octane; DAPI, 4′,6-diamidino-2-phenylindole; EDTA, Ethylenediaminetetraacetic acid; GPx, glutathione peroxidase; IF, immunofluorescence; MS, mass spectrometry; MT, microtubules; MN, motor neurons; NF, neurofilaments; PBS, phosphate buffered saline; Se-VI, sodium selenate; Se-IV, sodium selenite; Se-Met, seleno methionine; SD, Standard Deviation; TBS, Tris-buffered saline; TxTBS, Triton–X-100 TBS; TrxR, thioredoxin reductase; TUBA4A, tubulin α4A; WB, Western blot; WT, wild type

* Corresponding author at: Tullia Maraldi – via del Pozzo 71, 41124, Modena, Italy.
E-mail addresses: tullia.maraldi@unimore.it (T. Maraldi), francesca.beretti@unimore.it (F. Beretti), laura.anselmi@unimore.it (L. Anselmi), cinzia.franchin@unipd.it (C. Franchin), giorgio.arrigoni@unipd.it (G. Arrigoni), luca.braglia5@unibo.it (L. Braglia), jessica.mandrioli@unimore.it (J. Mandrioli), marco.vinceti@unimore.it (M. Vinceti), sandra.marmiroli@unimore.it (S. Marmiroli).
[1] Equal contributors

https://doi.org/10.1016/j.neuro.2019.09.015
Received 10 July 2019; Received in revised form 26 September 2019; Accepted 27 September 2019
Available online 01 October 2019
0161-813X/

the disease (Smith et al., 2014)(Pensato et al., 2015).

TUBA4A is ubiquitously expressed in all cell types, but at high levels in the nervous system (Rustici et al., 2012)(Smith et al., 2014). The expression of TUBA4A also increases with aging, possibly revealing why mutations in these genes cause later age disease phenotypes, unlike congenital tubulin mutations, which generate developmental disorders (Tischfield et al., 2011)(Hersheson et al., 2013).

Evidence has been provided that microtubule mediated deficits in axonal transport are a pivotal point for MNs survival in both sporadic and familial disease (Clark et al., 2016). However, it remains unclear if altered MT function is the cause, or consequence, of upstream initiating etiopathogenic mechanisms, such as mitochondrial-dependent energy depletion, excitotoxicity and calcium dysregulation and cellular oxidative stress (Ferraiuolo et al., 2011) (Peters et al., 2015).

While ROS are required for cytoskeletal remodeling and during axonal growth (Munnamalai and Suter, 2009)(Wilson and González-Billault, 2015), an excess ROS production can have harmful impacts on MTs (Landino et al., 2004), through multiple ways. For instance, the cellular redox status could be tightly joined with MT formation since ROS signals regulate the organization of MT and induce tubulin modifications (Livanos et al., 2014), as both α- and β- tubulin contain Cys residues that have the capacity to oxidize (Landino et al., 2007)(Wilson and González-Billault, 2015). Oxidative stress conditions due to an increased intracellular level of oxidized glutathione may alter the cytoskeleton organization and of its function leading to axon degeneration (Carletti et al., 2011). The interplay between these modifications and insults to MTs are not well understood, however, MTs may act as a site for mechanistic convergence, as they are affected by various pathogenic molecular mechanisms associated with neurodegeneration (Clark et al., 2016).

In humans, selenium, a trace element of both nutritional and toxicological interest, has been hypothesized to exert neurotoxicity, including a selective damage to motor neurons, thus inducing the onset of the human motor neuron disease ALS (Vinceti et al., 2014).

Se toxicity mechanisms have not been completely elucidated yet, but they are mainly ascribed to the generation of superoxide and hydrogen peroxide during reduction of active Se compounds (Misra et al., 2015)(Vinceti et al., 2018a). Several selenium species have been recently shown to be increased in cerebrospinal fluid of an ALS patient carrying the TUBA4A mutation, as was Se-Met in other patients affected by familial ALS, compared to referents, suggesting an involvement of some selenium species in the disease (Mandrioli et al., 2017).

The present study aims to investigate the mechanisms through which selenium compounds may affect cytoskeleton in a human neuron cell line and induce MTs interactome alterations, based on an *in vitro* experimental model of selenium toxicity we previously used (Maraldi et al., 2011).

2. Material and methods

2.1. Materials

Sodium selenite, sodium selenate, seleno-L-methionine, 2′,7′-dichlorofluorescin-diacetate (DCFH-DA), 2′,7′-dichlorofluorescein (DCF), 3-(4,5-dimethylthiazol-2-yl)-2,5-diphenyl tetrazolium bromide (MTT), 4′,6-diamidino-2-phenylindole dihydrochloride (DAPI), Igepal CA-630, orthovanadate, phenyl-methylsulfonyl fluoride (PMSF), N-tosyl-L-lysine chloromethyl ketone (TLCK), N-tosyl-L-phenylalanine chloromethyl ketone (TPCK), and were from Sigma-Aldrich (St. Louis, MO, USA).

Anti-goat, anti-mouse and anti-rabbit IgG conjugated to horseradish peroxidase and Western Blotting Luminol Reagent were purchased from Pierce (Rockford, IL, USA). A list of primary antibodies is reported in Table 1. Anti-MAP2 was from Cell Signaling Technology (Beverly, MA, USA), anti- nestin, anti-human mitochondria protein, anti-βtubulinIII were from Millipore (Temecula, CA, USA), anti-αtubulin4A was form Novus Biologicals (CO, USA), anti-GPx1, anti-TrxR1 and 2, anti-SOD1, anti-TIA-1, anti-Eif4G, anti-ubiquitin were from Santa Cruz Biotechnology (Santa Cruz, CA, USA), anti-HA, anti-actin, anti-tubulin and phalloidin were from Sigma-Aldrich (St Louis, MO, USA), anti-GSH was from Abcam (Cambridge, UK), anti-V5 was from Invitrogen (CA, USA) and anti-FUS was from Millipore (Temecula, CA, USA). Secondary antibodies for immunofluorescence were from Jackson ImmunoResearch Labs (West Grove, PA, USA). All the other chemicals and solvents were of the highest analytical grade.

Table 1
Antibodies list.

Antibody	Supplier
MAP2	Cell Signaling Technology (Beverly, MA, USA)
nestin	Millipore (Temecula, CA, USA)
human mitochondria protein	Millipore (Temecula, CA, USA)
βtubulinIII	Millipore (Temecula, CA, USA)
αtubulin4A	Novus Biologicals (CO, USA)
TIA-1	Santa Cruz Biotechnology (Santa Cruz, CA, USA)
Eif4G	Santa Cruz Biotechnology (Santa Cruz, CA, USA)
ubiquitin	Santa Cruz Biotechnology (Santa Cruz, CA, USA)
GPx1	Santa Cruz Biotechnology (Santa Cruz, CA, USA)
TrxR1	Santa Cruz Biotechnology (Santa Cruz, CA, USA)
TrxR2	Santa Cruz Biotechnology (Santa Cruz, CA, USA)
SOD1	Santa Cruz Biotechnology (Santa Cruz, CA, USA)
HA	Sigma-Aldrich (St Louis, MO, USA)
actin	Sigma-Aldrich (St Louis, MO, USA)
tubulin	Sigma-Aldrich (St Louis, MO, USA)
phalloidin	Sigma-Aldrich (St Louis, MO, USA)
GSH	Abcam (Cambridge, UK)
V5	Invitrogen (CA, USA)
FUS	Millipore (Temecula, CA, USA)

2.2. Cell cultures

SKNBE human neuroblastoma cells (from DSMZ, Germany) were grown in DMEM-F12 medium supplemented with 10% foetal bovine serum (FBS) (all EuroClone Ltd., UK), L-glutamine (2 mM), penicillin (50 UI/mL), streptomycin at 37 °C under a humidified 95% to 5% (vol/vol) mixture of air and CO_2. SKNBE were differentiated towards neuron cells treating with medium with 10% foetal bovine serum (FBS) supplemented with 10 μM retinoic acid for 1 week.

Human Embryonic Kidney 293 cells (HEK-293), obtained from DSMZ, were cultured as previously reported (Maraldi et al., 2009). In brief, cells were grown in DMEM-high glucose supplemented with 10% FBS.

2.3. Infection

TUBA4A overexpression on SKNBE cells was performed with specific human TUBA4A V5 tagged lentiviral expression plasmid (pLX304, DNASU, AZ, USA). Neuronal pre-differentiated SKNBE cells were transduced with 5 μg/ml polybrene (Sigma, USA) by lentiviral supernatant obtained in packaging hosts HEK-293 cells as described in the supplier's instruction manual. The medium was changed 48 h after infection maintaining differentiation, cells were selected with 2 μg/ml of blasticidin and treated with selenium compounds. Lentiviral pLKO empty vectors were used as the control.

2.4. Transfection

Transient TUBA4A overexpression on 293 T cells was obtained by polyethyleneimine (PEI) transfection using a 3:1 ratio of PEI (μg): total DNA (μg). Cells were transfected with empty vector as control, TUBA4A WT or TUBA4A mutants A383 T or R320C (DITTA) for 24 h.

2.5. ROS detection

To evaluate intracellular ROS levels, dichlorodihydrofluorescein diacetate (DCFH-DA) assay was performed as previously described (Casciaro et al., 2018). Cells were seeded in 96 well plate at density of 3000 cells/well, 6 replicates. The cells were treated with selenium compounds (sodium selenite, sodium selenate and seleno-methionine at 0.1, 0.5 and 0.5 μM respectively) for 4 days. Cell culture medium was removed and the 5 μM DCFH-DA was incubated in PBS glucose 5 mM for 30 min, 37 °C and 5% CO_2. The cell culture plate was read at 485 nm (excitation) and 535 nm (emission) using the Appliskan instrument (Thermo Fisher Scientific, Vantaa, Finland).

2.6. Cell viability assay

Viable cells treated with selenium compounds were evaluated by the MTT assay. Cells were incubated with 0.5 mg/mL MTT for 4 h at 37 °C, as previously reported (Lucarelli et al., 2002). At the end of the incubation, purple formazan salt crystals were dissolved by adding the solubilization solution (isopropanol, 0.1 M HCl). The absorption at 570 nm was measured on a multiwell plate reader (Appliskan, Thermo Fisher Scientific, Vantaa, Finland).

2.7. Immunofluorescence and confocal microscopy

For immunofluorescence analysis, cells treated with selenium compounds were processed as previously described (Guida et al., 2013). Cells were fixed in toto in 4% paraformaldehyde in PBS and permeabilized with 0.1% Triton X-100 in PBS for 10 min. After a treatment with 3% BSA in PBS for 30 min at room temperature, cells were incubated 1 h at room temperature with the primary antibodies diluted in PBS containing 3% BSA. After washing in PBS containing 3% BSA, the samples were incubated 1 h at room temperature with the secondary antibody diluted 1:200 in PBS containing 3% BSA (goat anti-rabbit FITC and donkey anti-mouse Cy5). After washing in PBS the samples were incubated for 5 min with DAPI, washed and then mounted with antifading medium (0.21 M DABCO and 90% glycerol in 0.02 M Tris, pH 8.0). Negative controls consisted of samples not incubated with the primary antibody. Confocal imaging was performed by a Nikon A1 confocal laser scanning microscope. The confocal serial sections were processed with ImageJ software to obtain three-dimensional projections. The image rendering was performed by Adobe Photoshop software.

2.8. Cell treatment and preparation of cell extracts

Cells were treated with selenium compounds and cell extracts were obtained as described (Naeem et al., 2015). Briefly, subconfluent cells were extracted by addition of modified RIPA buffer (20 mM Tris-Cl, pH 7.0; 1% Nonidet P-40; 150 mM NaCl; 10% glycerol; 10 mM EDTA; 20 mM NaF; 5 mM sodium pyrophosphate; and 1 mM Na_3VO_4) and freshly added Sigma Aldrich Protease Inhibitor Cocktail at 4 °C for 30 min. Lysates were sonicated, cleared by centrifugation and immediately boiled in SDS sample buffer or used for immunoprecipitation experiments, as described below. For GSH detection the lysates were separated by electrophoresis under nonreducing conditions.

2.9. Immunoprecipitation and western blot

Equal amounts of lysates, whose protein concentration was determined by the Bradford method, were loaded onto SDS-polyacrylamide gel, blotted on Immobilon-P membranes (Millipore, Billerica, MA, USA), and processed by Western blot with the indicated antibody. Immunoprecipitation was performed as reported (Maraldi et al., 2015). Equal amounts of precleared lysates, whose protein concentration was determined by the Bradford method, were incubated overnight with anti-V5, anti-GSH, anti-FUS or anti-HA (3 μg all). Then the samples were treated with 30 μL of 50% (v/v) of protein A/G agarose slurry (GE Healthcare Bio-sciences, Uppsala, Sweden) at 4 °C with gentle rocking for 1 h. Pellets were washed twice with 20 mM Tris-Cl, pH 7.0; 1% Nonidet P-40; 150 mM NaCl; 10% glycerol; 10 mM EDTA; 20 mM NaF; 5 mM sodium pyrophosphate, once with 10 mM Tris-Cl, pH 7.4, boiled in SDS sample buffer, and centrifuged. For GSH detection the IP were treated under nonreducing conditions. Supernatants were loaded onto SDS-polyacrylamide gel, blotted on Immobilon-P membranes and processed by Western blot with the indicated antibodies, detected by Supersignal substrate chemiluminescence detection kit (Pierce, Rockford, IL, USA). Quantitation of the signal was obtained by chemiluminescence detection on a Kodak Image Station 440CF and analysis with the Kodak 1D Image software. Primary antibodies were raised against the indicated molecules.

2.10. SDS-PAGE and protein digestion

Proteins immunoprecipitating with anti-V5 for each sample were eluted as decribed above and loaded onto 10% SDS-PAGE. Electrophoresis was allowed to proceed until proteins were tightly packed in a single band. Gels were then stained in the Coomassie brilliant blue solution (0.1% Coomassie blue in 10% acetic acid, 45% methanol) and shaken at room temperature for 1 h. The gels were destained by soaking for 2 h in destaining solution (10% acetic acid, 30% methanol) (Beretti et al., 2018). In gel trypsin digestion was performed as previously reported (Resmini et al., 2017). Briefly, each gel band was divided in small pieces that were treated with solution A (1:1 mixture of acetonitrile: 100 mM ammonium bicarbonate) for 30 min and then dried under vacuum. Proteins were then subjected to reduction of disulfide bonds by 10 mM DTT at 56 °C for 1 h. Alkylation of cysteine residues was performed with 55 mM iodoacetamide for 45 min at room temperature in the dark. Before trypsin digestion, the rehydration and dehydration steps were again performed with solution A and samples were finally dried under vacuum. Digestion was performed by incubating the dry gel slices with 40 μL of sequencing grade modified trypsin (12.5 ng/μL in 50 mM NH_4HCO_3, Promega) at 37 °C, overnight. Peptides were extracted from the gels with 100 μL of acetonitrile/0.1% formic acid (3 times) and samples were dried under vacuum and stored at −20 °C until LC–MS/MS analysis was performed.

2.11. Mass spectrometry and data analysis

Each sample was dissolved in 30 μL of formic acid 0.1% and 3 μL of this solution was injected into a nano-LC system (Ultimate 3000, Dionex – Thermo Fisher Scientific) coupled online to a LTQ-Orbitrap XL mass spectrometer (Thermo Fisher Scientific). Peptides were loaded into a 11 cm pico-frit capillary column (New Objective) packed in house with C18 material (Aeris Peptide 3.6 μm XB-C18, Phenomenex) and separated using a linear gradient of acetonitrile/0.1% formic acid from 3% to 40% in 40 min. The mass spectrometer operated with a Top4 data dependent acquisition method, performing a full scan at 60,000 resolution in the Orbitrap, followed by the fragmentation in the linear trap of the four most intense ions.

Raw data files were analyzed with the software package MaxQuant (Cox and Mann, 2008) (Tyanova et al., 2016). MS/MS spectra were analyzed with the search engine Andromeda (Cox et al., 2011) against the Human section of the Uniprot database (version June 2018) and against a database of contaminants commonly found in proteomics experiments. The search parameters were set as follows: trypsin was selected as enzyme with one missed cleavage allowed; carbamidomethylation (C) was specified as fixed modification while, oxidation (M) as variable modification. Results were filtered at a False Discovery Rate (FDR) of 0.01, both at the peptide and protein level. Only proteins identified with at least 2 independent peptides were considered as a

significant hit. The parameter "Intensity" calculated by the software and normalized based on the total amount of TUBA4A was used to estimate the abundance of the proteins across the different samples.

2.12. Bioinformatic analysis

The lists of identified proteins were subjected to PANTHER classification system, version 9.0 (http://www.pantherdb.org/), for understanding biological context of the identified proteins and their involvement in biological pathways (Beretti et al., 2018). The list of UniProt Accession number was uploaded and mapped against reference Homo sapiens dataset to extract and summarize molecular functions, biological processes and the class of proteins.

2.13. Statistical analysis

In vitro experiments were performed in triplicate. For quantitative comparisons, values were reported as mean ± SD based on triplicate analysis for each sample. To test the observed differences among the study groups Student's *t*-test or One-way Anova with Bonferroni post hoc test were applied. Statistical analysis and plot layout were obtained by using GraphPad Prism® release 5.0 software.

3. Results

3.1. Effect of selenium treatments on ROS content and cell morphology

We previously demonstrated that the selenium compounds sodium selenate (Se-VI), sodium selenite (Se-IV) and seleno methionine (Se-Met), at a concentration of 0.5, 0.1 and 0.5 μM respectively, give rise to a significant increase in ROS amount (150%) already at 1 h treatment up to 18 h in SKNBE cells (Maraldi et al., 2011). Here we decided to follow the effect of selenium on ROS levels at longer times, namely 24 h, 4 days and 1 week, monitoring in parallel viability parameters and cell morphology. The effects at 24 h was similar to that observed at 18 h (data not shown). Conversely, starting from the day 4 of treatment we noticed a further increase in the ROS amount maintaining a cell viability at around 70%. Fig. 1A shows the ratio between the intracellular DCF-reactive species/MTT values, highlighting the permanence of high ROS levels (average 200%) leading to a redox unbalance and thus an oxidative stress status.

The accumulation of ROS induced evident morphological modifications: in particular the presence of long neurites, typical of neuron cells, dramatically decreased upon selenium treatments. The graph of Fig. 1B shows that with all the selenium compounds the number of cells with long cytoplasmic extroflessions is less than one third compared to the untreated sample (control).

Similarly to the 24 h of selenium treatments previously demonstarted, after 4 days cells exhibited more intense bands recognized by the anti-GPx1 (glutathione peroxidase 1), anti-TrxR (thioredoxin reductase) both the cytosolic (1) and the mitochondrial isoform (2) (Fig. 1C), suggesting an involvement of selenium in the synthesis of selenium-containing enzymes. However, Se administration decreases expression of other antioxidant enzymes such as superoxide-dismutase 1 (SOD1) (Fig. 1C).

3.2. Effect of selenium treatments on the cytoskeleton

Giving the importance of cytoskeletal proteins in the neuron morphology and functionality, we investigated by immunofluorescence the impact of selenium on the distribution and the expression of microfilament, intermediate filament and microtubule molecules.

The staining of actin was consistent with that of total αtubulin, showing short neurites in treated samples (Fig. 2), supporting the data observed by phase contrast microscopy (graph of Fig. 1B). Moreover, the distribution of mitochondria in cytoplasmic extroflessions was affected by selenium, as showed by magnified images and graph. In fact, the presence of mitochondria was limited to the cell body area in the samples treated with Se-VI, Se-IV and Se-Met.

As neuroblastoma SKNBE cells were treated with neurodifferentiating medium before and during selenium treatments as shown in Supp Fig. 1, we next focused our attention on the typical neuronal cytoskeletal molecules, βtubulin III, MAP2 and nestin, that are involved in neurodifferentiation. Fig. 3 shows IF images revealing that the whole cytoskeleton expression of differentiating cells is affected, although to a greater extent in the case of MTs.

3.3. Tubulin Alpha 4a interactome: effect of selenium compounds

Since mutations on tubulin isoform TUBA4A are sufficient to cause a familial, albeit rare, form of ALS disease, we focused on MTs, overexpressing wild type (WT) TUBA4A V5-tagged in SKNBE cells in order to explore the possible effect of selenium on this specific isoform interactome. Fig. 4A shows that our experimental condition allowed to obtain a good overexpression efficiency, since around 50% of cells are positive for the tag (V5) staining. Immunoprecipitation procedure with anti-V5 was carried out for all the cell lysates and then IP-pellets were processed for protein identification and quantification with mass spectrometry. Interestingly, the identification and the quantity comparison among selenium treated samples *vs* control, obtained from LC–MS/ MS analysis, revealed that at least 20 proteins increase (more than 5 times) their interaction with TUBA4A following selenium treatments. These identified proteins were classified using Gene Ontology terms (http://geneontology.org/). The PANTHER GO analysis, showed in the pie charts of Fig. 4B, highlighted nucleic acid binding proteins (violet slice) as the category with the highest increase. Interestingly, some of the proteins listed in this category are known to be typically involved in the ALS pathogenesis, such as fused in sarcoma (FUS) and TIA-1. We therefore performed co-immunoprecipitation experiments in order to validate this result.

In Fig. 5A SKNBE total cell extracts immunoprecipitated with anti-V5 and immunoblotted with anti-FUS and anti-TIA-1 are shown. The treatments with selenium compounds enhanced the interaction of both these proteins with TUBA4A. The detection of V5 was performed in order to control that comparable levels of V5 protein were immunoprecipitated, and the graphs show the IP gray level of each protein normalized to the relative total lysate. Similarly, cell extracts immunoprecipitated with anti-FUS, and then immunoblotted with anti-TUBA4A and anti-TIA-1, display (in Fig. 5B) the same trend confirming the above result.

Since FUS is a DNA/RNA binding protein known to relocalize in the cytoplasm of neurodegenerating cells of ALS patients, we then investigated by immunofluorescence experiments the intracellular distribution of FUS. Images of Fig. 5C demonstrate a mislocalization of FUS in some cells of treated samples. Indeed, FUS appeared not only into the nuclei, as demonstrated by the overlap of DAPI signal with the one of FUS, but also in the cytoplasmic area, where its higher interaction with a cytoplasmic cytoskeletal protein such as TUBA4A can therefore take place. This aspect is consistent with the one of FUS mutated dependent ALS cases.

3.4. Effect of selenium on post-translational modifications of TUBA4A

We hypothesized that the oxidative stress induced by selenium treatments could trigger TUBA4A post-translational modification on Cys, a mechanism involved in ALS etiopathogenesis. Therefore we tested the status of glutathionylation of SKNBE cells, treated or not with selenium for 16 h, by immunoprecipitation experiments in non-reducing condition. Fig. 6A shows that TUBA4A is more glutathionylated in the presence of selenium compounds. Remarkably, this effect was mimicked also by HEK293 cells expressing TUBA4A with Arginine mutated to Cysteine, although it is detectable also in cells carrying another

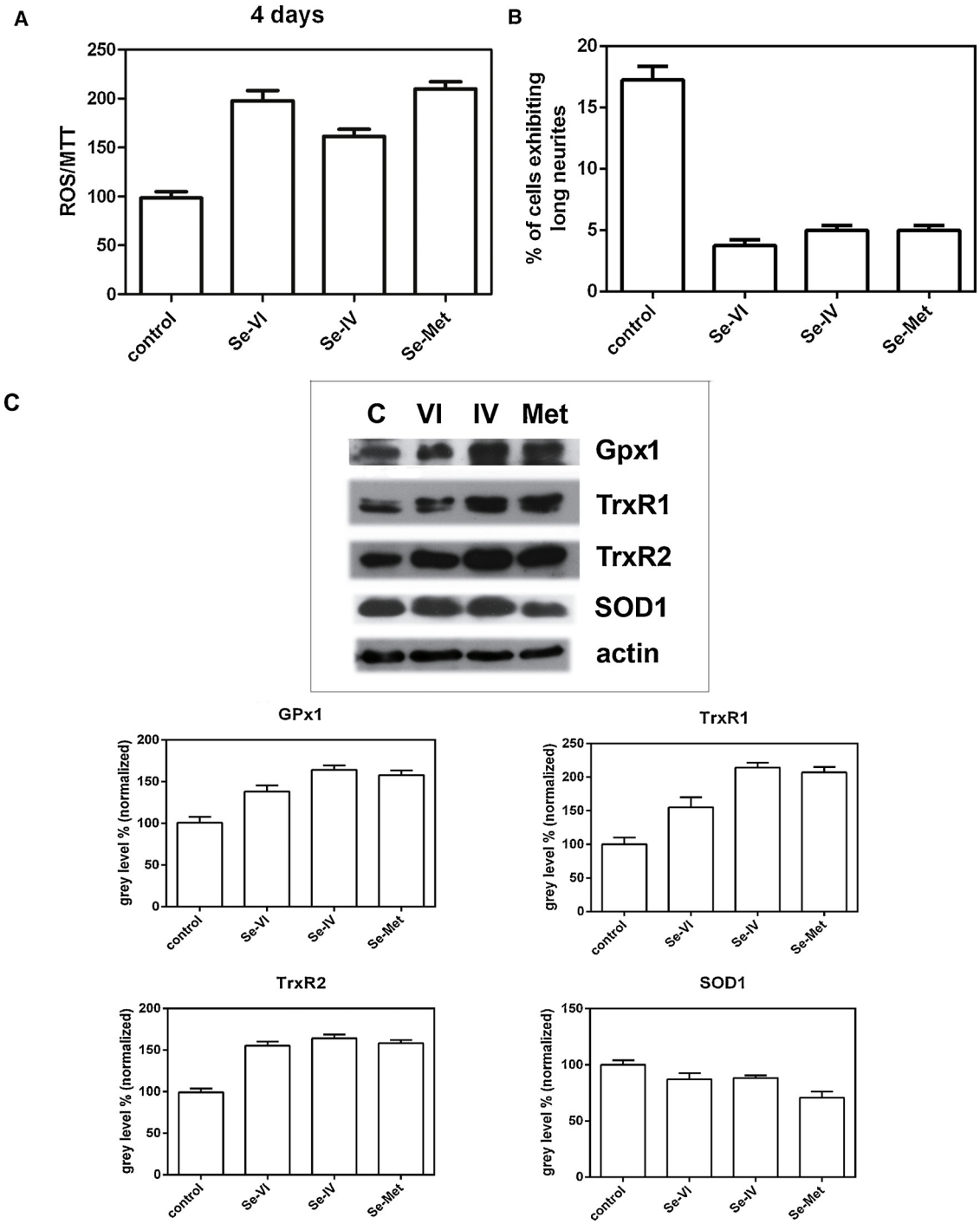

Fig. 1. Effect of selenium supplementation on ROS content and cell morphology of SKNBE cells.
A - Cells were incubated for 4 days with 0.5 μM sodium selenate (Se-VI), 0.1 μM sodium selenite (Se-IV), and 0.5 μM selenomethionine (Se-Met). ROS content was measured with DCFH-DA as described in the Material and Methods section. The graph shows the DCF fluorescence (ROS) normalized to the MTT values. P values are 0.0002, 0.0006, 0.0001 for Se-VI, Se-IV and Se-Met respectively. B – The graph represents the percentage of cells, incubated or not for 4 days with selenium compounds, showing neurite length that doubles the size of cell bodies. Results are expressed as means ± SD of three independent experiments, each performed in triplicate. P values are 0.0001, 0.0001, 0.0001 for Se-VI, Se-IV and Se-Met respectively. C - Cells treated as in A were lysates and western blot was performed as described in the Materials and Methods section. A representative immunoblot revealed for anti-GPx1, anti-TrxR1 and 2, anti-SOD1 and anti-actin is showed. Relative amounts determined by scanning densitometry analysis are in arbitrary units and compared to the control. P values for GPx1 are 0.0006 for Se-VI and 0.0001 for Se-IV and Se-Met. P values for TrxR1 are 0.0011 for Se-VI and 0.0001 for Se-IV and Se-Met. For TrxR2 are 0.0001 for all the treatments compared to the control. For SOD1 P values are 0.0468, 0.0801 and 0.0003 for Se-VI, Se-IV and Se-Met respectively compared to the control.

ALS-related mutation, T383A (Fig. 6B).

Since we have noticed that TUBA4A expression decreased following selenium treatments in total lysates (Fig. 5B), we finally investigated the ubiquitination level of TUBA4A in SKNBE treated with sodium selenite for 16 h, with or without MG-132 for 5 h, an inhibitor of proteasome activity, as a positive control. In fact, MG-132 provoked accumulations of ubiquitinated TUBA4A and a similar result was obtained with selenite treatment. Therefore addition of selenite not only triggers

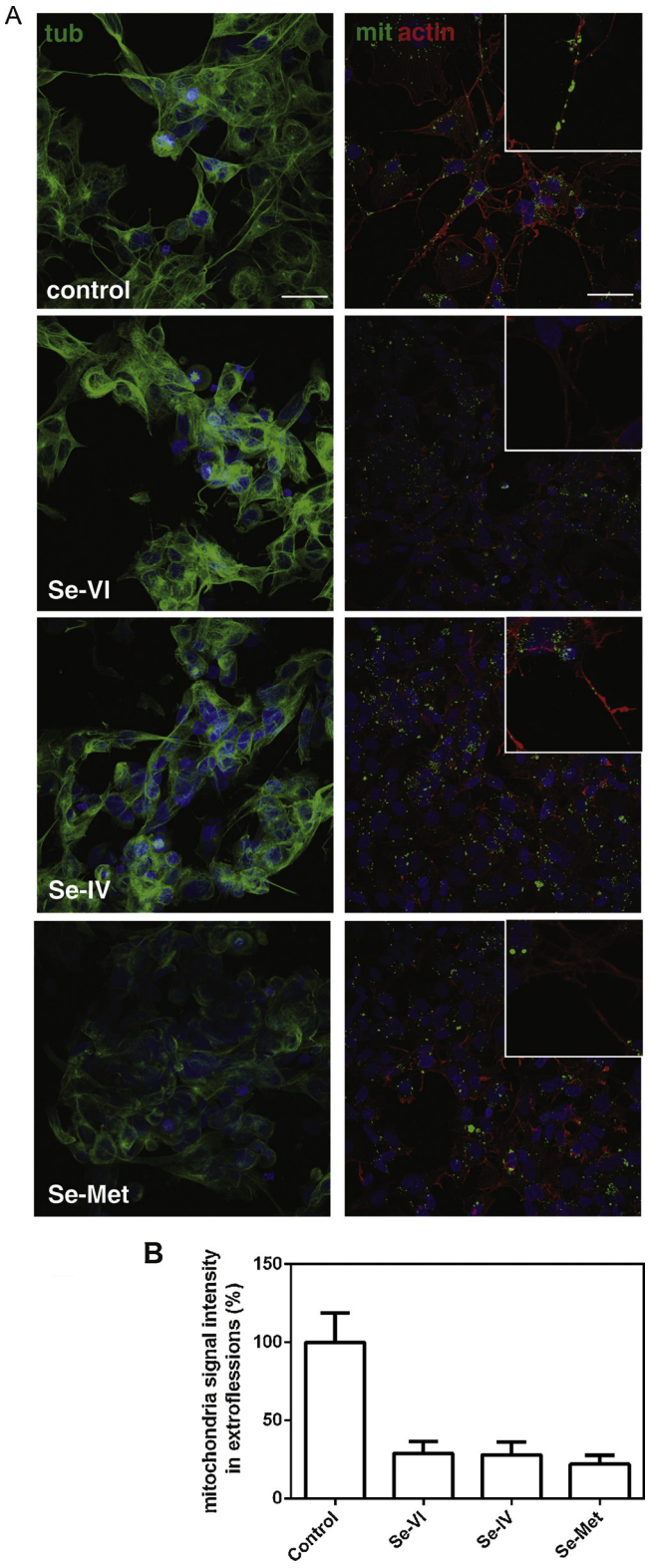

Fig. 2. Effect of selenium supplementation on cytoskeleton and mitochondrial distribution in SKNBE cells.
Representative images showing DAPI (blue) and tubulin (green) or mitochondrial protein (green) and phalloidin (actin, red) signals of SKNBE incubated or not for 4 days with selenium compounds. Scale bar = 20 μm. In white squares are shown representative doubled magnification images. The graph represents the normalized green fluorescence intensity of mitochondrial protein in the extroflessions. P values are 0.0001 for Se-VI, Se-IV and Se-Met.

glutathionylation of TUBA4A, but also enhances its ubiquinination (Fig. 6C). Whether these two effects are independent or linked in some hierarchical way remains to be determined.

4. Discussion

An extremely diverse set of biochemical processes has been implicated in ALS disease, that may be grouped in RNA metabolism and translational biology; protein quality control; cytoskeletal integrity and trafficking; mitochondrial function and transport; and oxidative stress (Cook and Petrucelli, 2019). This suggests, therefore, that several pathways of toxicity are strictly intertwined and could cooperate in the pathogenesis of ALS. The increase of ROS (Beal, 2002) and reduction of TUBA4A protein was confirmed in brain cortex tissue of fALS and sALS patients, and led to motor axon defects in an *in vivo* model. The discovery of a TUBA4A depolymerization and degradation pathogenic cascade in both fALS and sALS suggest that TUBA4A alterations may occur in a large proportion of ALS cases (Helferich et al., 2018). In this study we tried to assess the possible existence of crosslinks among selenium toxicity, oxidative stress, neurotubule damage in the framework of ALS pathogenesis.

The important role played by redox stress in ALS pathology was clearly demonstrated by the high levels of protein carbonyl and nitrotyrosine modifications found in the spinal cords of ALS patients and mouse models of familial ALS (Beal, 2002). Neurons are highly vulnerable to oxidative stress and oxidation of cytoskeletal proteins is considered one of the first steps of neurodegeneration. Selenium involvement in ALS has been suggested on the basis of epidemiological studies (Vinceti et al., 2018a)(Vinceti et al., 2018b), *in vitro* investigations, and veterinary studies in which selenium induced a selective toxicity against motor neurons (Vinceti et al., 2014). In this context, some elevated selenium species levels found in cerebrospinal fluid of ALS patients with both the sporadic (Vinceti et al., 2013) and the familial form of the disease (Mandrioli et al., 2017) suggested an interaction between this environmental factor and a specific genetic background possibly triggering the disease onset. Moreover, since oxidative stress has long been recognized as a major toxic effect of selenium species, the evidence of their pro-oxidant effect on neuronal cells even at low concentrations is particularly relevant (Maraldi et al., 2011) (Jablonska and Vinceti, 2015). Here we further demonstrated the maintenance and the additional increase of reactive oxygen species due to the selenium compounds long exposure, indicating that the intracellular redox machinery is definitively affected, as well as the cell morphology, through remodelling of cytoskeletal elements such as the MT.

Perturbations in MT and microtubule associated protein functions have been implicated in a range of neurodegenerative diseases (Penazzi et al., 2016), including ALS (Baird and Bennett, 2013)(Smith et al., 2014). In ALS, MT dysfunction has been hypothesized to influence predominantly the physical length of the axon in affected MNs, as well as alterations to MTs cause defects on axonal transport (Millecamps and Julien, 2013). In our study, we observed that selenium treatments induced a dramatic decrease in axon of SKNBE cells, causing an altered distribution of mitochondria, a clear indication that also the axonal transport is compromised.

MTs also interact with other cytoskeletal networks, such as the neuronal microfilament actin, and the neuronal specific NFs which are known to influence MT structure and function. Our results show that during the differentiating process of SKNBE cells, the selenium presence negatively influenced tubulinβIII expression more than the one of the specific NF nestin. TubulinβIII, indeed, may be critical in the response of neuronal cells to stress, using sulfhydryl groups to scavenge ROS and defend neuronal cells against oxidative stress.

The modifications to neuronal MTs include tubulin tyrosination, acetylation, polyamination, glutathyonilation, glutamylation and glycylation (Janke and Kneussel, 2010) (Magiera and Janke, 2014).

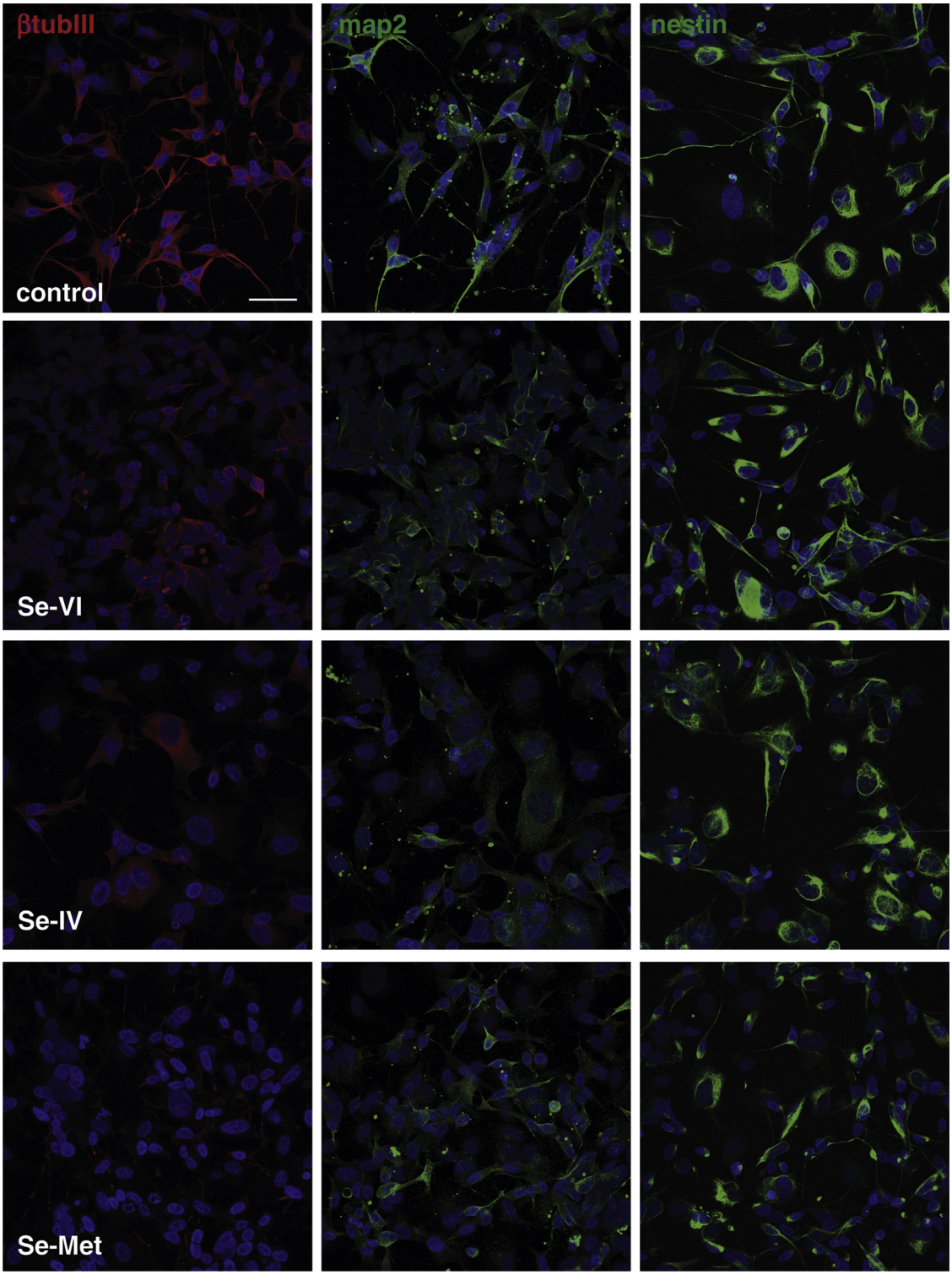

Fig. 3. Effect of selenium supplementation on neuronal cytoskeleton.
Representative images showing DAPI (blue) and βtubulinIII (red), MAP2 (green) or nestin (green) signals of SKNBE incubated or not for 4 days with selenium compounds. Scale bar = 20 μm.

However, in oxidative stress conditions the increase of intracellular GSSG level may induce a cytoskeletal dysfunction and ultimately an axonal degeneration through protein glutathionylation that is a critical event in the redox regulation of protein function and constitutes a sensor of tissue oxidative stress in patho-physiological conditions (Landino et al., 2004). It is therefore conceivable to regard the neuronal cytoskeleton as a primary target for post-translational modification by GSSG (Carletti et al., 2011).

Starting from the recent identification of tubulin gene mutations (TUBA4A) and their impact on MT function (Smith et al., 2014), we focused our attention on the effect of selenium compounds on TUBA4A and glutathionylation. In good agreement, we report here for the first time that TUBA4A undergoes this post-translational modification after exposure to selenium compounds that is already detectable at 16 h.

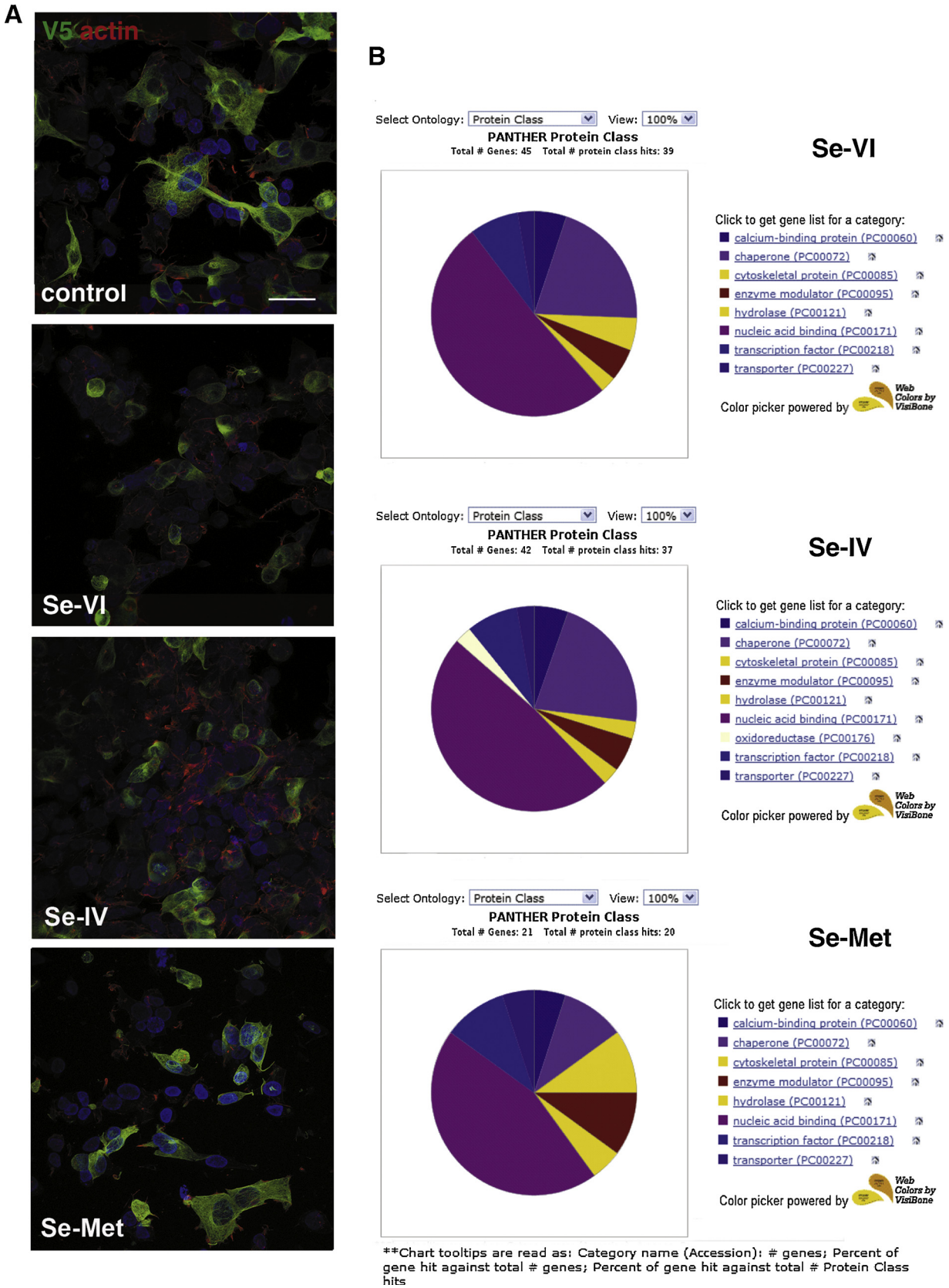

Fig. 4. Effect of selenium supplementation on TUBA4A interactome.
A – SKNBE cells, overexpressing V5 tagged TUBA4A, were incubated or not for 4 days with selenium compounds. Representative images showing DAPI (blue), V5-TUBA4A (green) and phalloidin (actin, red) signals are shown. Scale bar = 20 μm. B – SKNBE overexpressing V5 tagged TUBA4A, treated or not with selenium compounds, were lysated and V5-immunoprecipitating proteins were analyzed by MS, described in the Material and Methods section. Panther GO-Slim classification shown in pie charts of differentially (more than 5 times) interacting proteins in Se-VI, Se-IV, Se-Met *vs* control SKNBE cells according to their protein class. The lists include 39, 37, 20 proteins for Se-VI, Se-IV, Se-Met respectively.

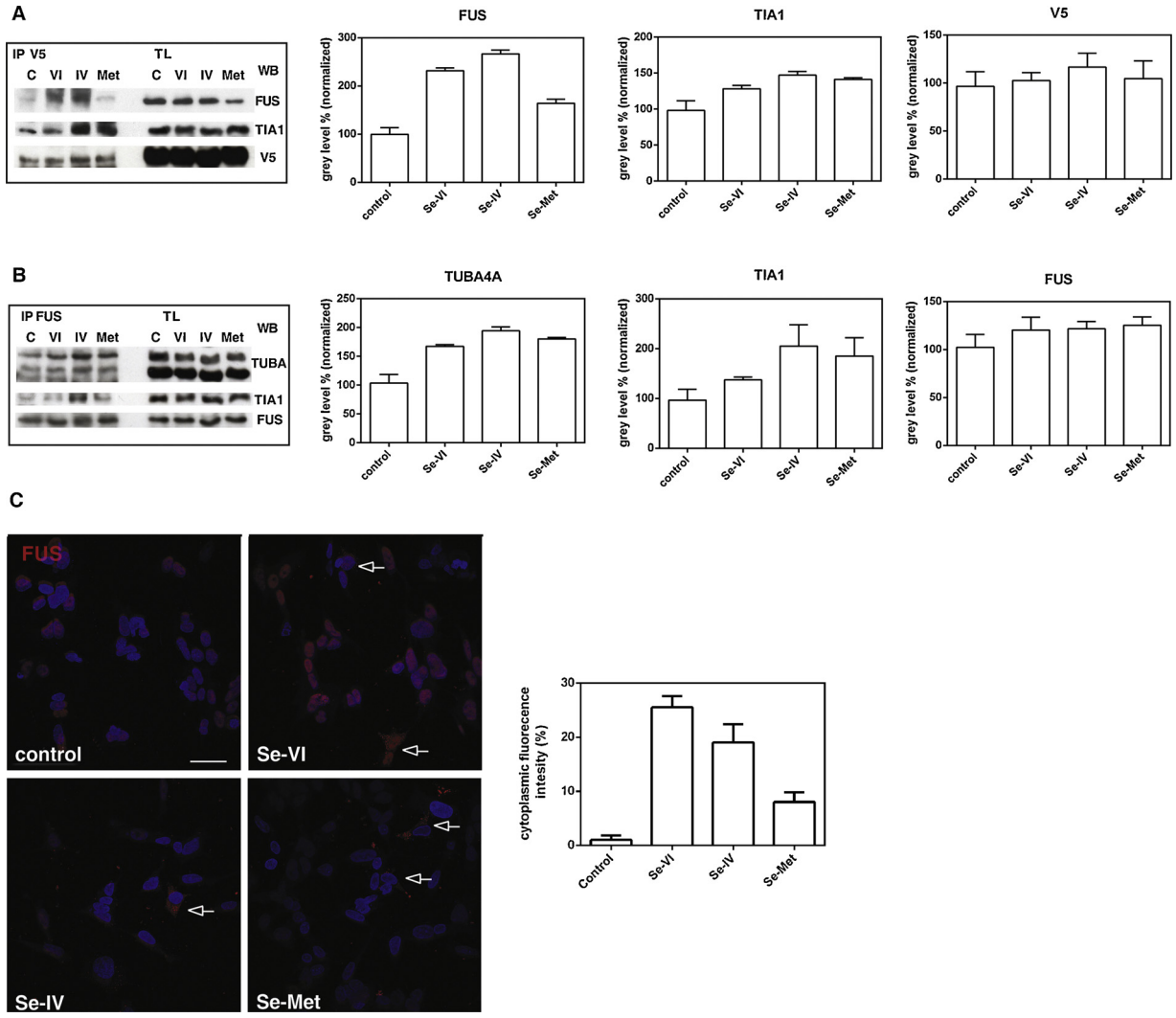

Fig. 5. Effect of selenium supplementation on TUBA4A interaction with the nucleic acid binding protein FUS.
A - Western blot analysis of total lysate (TL) and immunoprecipitation (IP) experiment with anti-V5 antibody of SKNBE, overexpressing V5 tagged TUBA4A treated or not with selenium compounds, then revealed with anti-FUS, anti-TIA-1 and anti-V5 antibodies. The graph shows the densitometry of each IP bands normalized to the relative TL. P values for FUS are 0.0001 for Se-VI, Se-IV and Se-Met. P values for TIA1 are 0.003 for Se-VI, and 0.0001 for Se-IV and Se-Met. B – The same samples were immnunoprecipitated with anti-FUS and revealed with anti-TUBA4A, anti-TIA-1 and anti-FUS antibodies. Data are representative of three independent experiments. The graphs show the densitometry of each IP bands normalized to the relative TL. P values for TUBA4A are all 0.0001 for Se-VI, Se-IV and Se-Met compared to the control. P values for TIA1 are 0.005 for Se-VI, and 0.0005 for Se-IV and Se-Met. C - Representative images showing DAPI (blue) and FUS (red) signals of SKNBE incubated or not for 4 days with selenium compounds. Arrows indicate FUS presence in the cytoplasm. Scale bar = 20 μm. The graph represents the normalized red fluorescence intensity of FUS in the cytoplasm. P values are 0.0001 for Se-VI, Se.IV and 0.0004 for Se-Met.

What's more, the same treatment triggered also TUBA4A ubiquitination, an event known to promote protein degradation through the proteasome-lysosome machinery. Whether glutathionylation of TUBA4A is a mandatory modification priming TUBA4A for subsequent ubiquitination and degradation remains to be determined. However, it is worth to underline that we observed an overlapping modification of TUBA4A carrying the R to C point mutation (R320C). As this mutation has been recently discovered in a patient affected by ALS (Smith et al., 2014), we consider our finding as particularly deserving further investigation.

Since glutathionylation, like protein phosphorylation, can control enzyme activities, modify transcription profiles and change protein-protein interactions, thereby altering their function (Sun et al., 2012) (Cooper et al., 2011), we then investigated also the modification of TUBA4A interactome. Our finding highlights a general positive effect of selenium on TUBA4A binding to nucleic acid binding proteins, such as fused in sarcoma (FUS). Nuclear DNA/RNA binding protein FUS is involved in various aspects of gene expression through mRNA metabolism and mRNA transport (Kamelgarn et al., 2018). Interestingly, mutations in the FUS gene were discovered to contribute to a subset of familial ALS (Kwiatkowski et al., 2009) where mutant FUS accumulates in the cytoplasm, due to a loss of the nuclear import. In turn, cytoplasmic accumulation of FUS forms stable ribonucleoprotein granules, which can lead to inclusion bodies and possibly contribute to neurotoxicity (Yang et al., 2015). It is therefore interesting that, after selenium exposure, a FUS accumulation in the cytoplasm occurred, suggesting that this element affect different aspects involved in ALS pathogenesis that are, in some ways, linked with oxidative stress status. In response to oxidative stress, neurons can form transient stress granules SGs, and defects in SG dynamics can accelerate neurodegeneration (Wolozin, 2014). As such, SGs have been observed in Alzheimer's disease, ALS, fronto-temporal dementia (FTD), spinocerebellar ataxia, and Huntington's disease (Dobra et al., 2018). Although SGs regulate redox levels, SG formation is in turn itself differently controlled by various types of oxidative stress. Cytoskeleton is involved in SG dynamics, especially the microtubules and microtubule-associated motor proteins play a pivotal

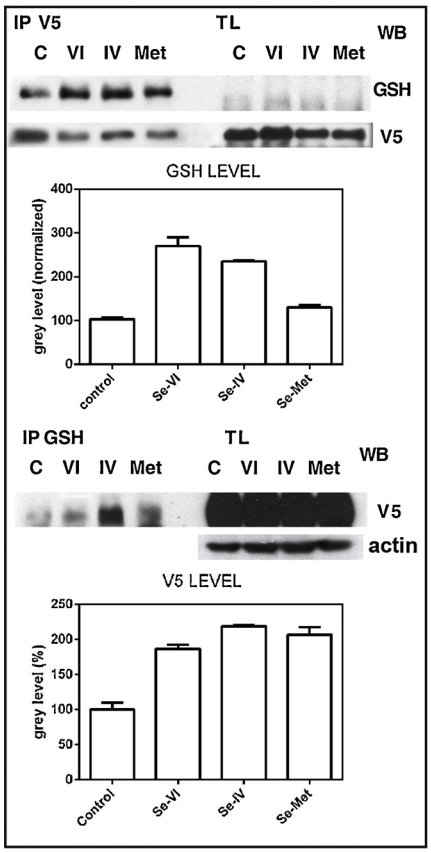

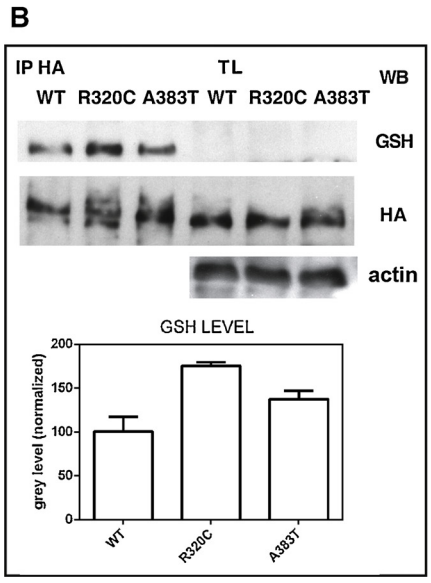

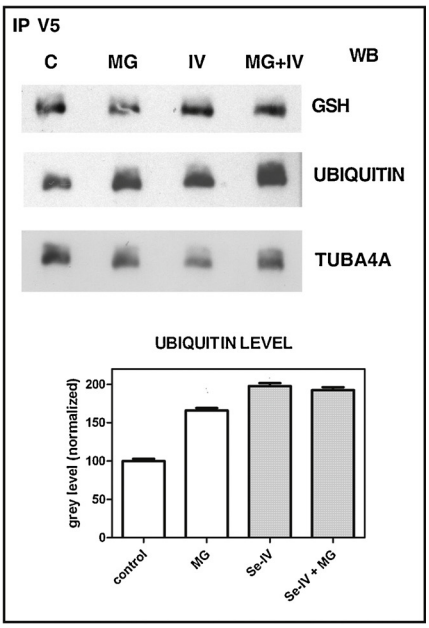

Fig. 6. Effect of selenium supplementation on TUBA4A posttranslational modifications.
A - Western blot analysis of total lysate (TL) and immunoprecipitation (IP) experiment, in not reducing condition, with anti-V5 antibody of SKNBE, overexpressing V5 tagged TUBA4A treated or not with selenium compounds, then revealed with anti-GSH, and anti-V5 antibodies. Data are representative of three independent experiments that are shown in the graph displaying gray levels in %, normalized to the immunoprecipitated protein (V5). P values are 0.0014, 0.0002, 0.0017 for Se-VI, Se.IV and Se-Met respectively. The same samples were immunoprecipitated with anti-GSH and revealed with anti-V5 and anti-actin antibodies. The normalization is not applicable for IP anti-GSH. P values are 0.0012, 0.0001, 0.0203 for Se-VI, Se.IV and Se-Met respectively. B – Western blot analysis of total lysate (TL) and immunoprecipitation (IP) experiment, in not reducing condition, with anti-HA antibody of HEK293 cells, overexpressing HA tagged TUBA4A mutated in R320C or A383 T. The graph shows densitometric analysis of IP revealed with anti-GSH normalized to HA signals. Actin bands are shown for TL samples. P values are 0.0052, 0.108 for R320C and A383 T respectively. C - Western blot analysis of total lysate (TL) and immunoprecipitation (IP) experiment, in not reducing condition, with anti-V5 antibody of SKNBE, overexpressing V5 tagged TUBA4A treated or not with selenium selenite and/or MG132, then revealed with anti-GSH, anti-ubiquitin and anti- TUBA4A antibodies. The graph shows densitometric analysis of ubiquitin normalized to TUBA4A signals. P values are all 0.0001.

role in several aspects of granule formation (Chen and Liu, 2017).

Remarkably, many of the proteins involved in the pathogenesis of above mentioned disorders are present in SGs, for example the disease-causing forms of FUS, hnRNPA1, SMN, Tau and TDP-43, and the SG assembly promoting protein TIA1 (Chung et al., 2018). The identification of TIA1 mutations in ALS/FTD strengthens the role of RNA metabolism and SG dynamics in ALS/FTD pathogenesis (Mackenzie et al., 2017). For these reasons, it was not surprising for us to notice a greater interaction of TUBA4A also with TIA1 in selenium treated samples.

Since cytoplasmic SGs are involved in facilitating stress responses and for preventing the accumulation of misfolded proteins (Chen and Liu, 2017), the observations of the higher ubiquitination level of TUBA4A and its content decrease after selenium treatment are consistent with the hypothesis of proteasome degradation pathway. However, although it is clear that both glutathionylation and ubiquitination of TUBA4A can be modulated by selenium compounds, further investigation is needed to establish whether they occur as independent events downstream of selenium exposure or if they sequentially lay on a vertical axis of post-translational modifications. Furthermore, to

conclusively link settle a mechanistic hypothesis linking our observations to the pathophysiology of ALS it would be important to get confirmation that also point mutation at cysteine, or other residues involved in this disease, affects ubiquitination similar to selenium.

5. Conclusions

These data indicate that low concentrations of selenium compounds induce redox imbalance as well as MT dysfunction in neuronal cells, two mechanisms which might play a role in ALS etiopathogenesis. These findings can help to understand why MTs are considered a site for mechanistic convergence involved in the etiopathogenesis of some neurodegenerative diseases, and strengthen the hypothesis that overexposure to environmental selenium may represents a risk factor for ALS in humans.

Authors' contributions

TM, performed IF experiments, acquisition and interpretation of data and drafting the manuscript; FB, performed most of experimental data; LB, LA, performed transfection experiment; CF, GA, performed MS experiments; JM, revision of the manuscript critically for important intellectual content; interpretation of data and revision of the manuscript critically for important intellectual content; MV, revision of the manuscript critically for important intellectual content.

All authors read and approved the final manuscript.

Financial support and acknowledgment

This work was supported by the grant 2016 from Fondazione di Vignola, Italy..

Declaration of Competing Interest

Author Disclosure Statement: all the authors report no conflicts of interest.

Appendix A. Supplementary data

Supplementary material related to this article can be found, in the online version, at doi:https://doi.org/10.1016/j.neuro.2019.09.015.

References

Baird, F.J., Bennett, C.L., 2013. Microtubule defects & neurodegeneration. J. Genet. Syndr. Gene Ther. 4, 203. https://doi.org/10.4172/2157-7412.1000203.

Beal, M.F., 2002. Oxidatively modified proteins in aging and disease. Free Radic. Biol. Med. 32, 797–803.

Beretti, F., Zavatti, M., Casciaro, F., Comitini, G., Franchi, F., Barbieri, V., La Sala, G.B., Maraldi, T., 2018. Amniotic fluid stem cell exosomes: therapeutic perspective. BioFactors 44, 158–167. https://doi.org/10.1002/biof.1407.

Carletti, B., Passarelli, C., Sparaco, M., Tozzi, G., Pastore, A., Bertini, E., Piemonte, F., 2011. Effect of protein glutathionylation on neuronal cytoskeleton: a potential link to neurodegeneration. Neuroscience 192, 285–294. https://doi.org/10.1016/j.neuroscience.2011.05.060.

Casciaro, F., Beretti, F., Zavatti, M., McCubrey, J.A., Ratti, S., Marmiroli, S., Follo, M.Y., Maraldi, T., 2018. Nuclear Nox4 interaction with prelamin A is associated with nuclear redox control of stem cell aging. Aging (Albany N. Y.) 10, 2911–2934. https://doi.org/10.18632/aging.101599.

Chen, L., Liu, B., 2017. Relationships between stress granules, oxidative stress, and neurodegenerative diseases. Oxid. Med. Cell. Longev. 2017, 1809592. https://doi.org/10.1155/2017/1809592.

Chung, C.G., Lee, H., Lee, S.B., 2018. Mechanisms of protein toxicity in neurodegenerative diseases. Cell. Mol. Life Sci. 75, 3159–3180. https://doi.org/10.1007/s00018-018-2854-4.

Clark, J.A., Yeaman, E.J., Blizzard, C.A., Chuckowree, J.A., Dickson, T.C., 2016. A case for microtubule vulnerability in amyotrophic lateral sclerosis: altered dynamics during disease. Front. Cell. Neurosci. 10, 204. https://doi.org/10.3389/fncel.2016.00204.

Cook, C., Petrucelli, L., 2019. Genetic convergence brings clarity to the enigmatic red line in ALS. Neuron 101, 1057–1069. https://doi.org/10.1016/j.neuron.2019.02.032.

Cooper, A.J., Pinto, J.T., Callery, P.S., 2011. Reversible and irreversible protein glutathionylation: biological and clinical aspects. Expert Opin. Drug Metab. Toxicol. 7, 891–910. https://doi.org/10.1517/17425255.2011.577738.

Cox, J., Mann, M., 2008. MaxQuant enables high peptide identification rates, individualized p.p.b.-range mass accuracies and proteome-wide protein quantification. Nat. Biotechnol. 26, 1367–1372. https://doi.org/10.1038/nbt.1511.

Cox, J., Neuhauser, N., Michalski, A., Scheltema, R.A., Olsen, J.V., Mann, M., 2011. Andromeda: a peptide search engine integrated into the MaxQuant environment. J. Proteome Res. 10, 1794–1805. https://doi.org/10.1021/pr101065j.

Dobra, I., Pankivskyi, S., Samsonova, A., Pastre, D., Hamon, L., 2018. Relation between stress granules and cytoplasmic protein aggregates linked to neurodegenerative diseases. Curr. Neurol. Neurosci. Rep. 18, 107. https://doi.org/10.1007/s11910-018-0914-7.

Ferraiuolo, L., Kirby, J., Grierson, A.J., Sendtner, M., Shaw, P.J., 2011. Molecular pathways of motor neuron injury in amyotrophic lateral sclerosis. Nat. Rev. Neurol. 7, 616–630. https://doi.org/10.1038/nrneurol.2011.152.

Guida, M., Maraldi, T., Resca, E., Beretti, F., Zavatti, M., Bertoni, L., La Sala, G.B., De Pol, A., 2013. Inhibition of nuclear Nox4 activity by plumbagin: effect on proliferative capacity in human amniotic stem cells. Oxid. Med. Cell. Longev. 2013, 1–12. https://doi.org/10.1155/2013/680816.

Helferich, A.M., Brockmann, S.J., Reinders, J., Deshpande, D., Holzmann, K., Brenner, D., Andersen, P.M., Petri, S., Thal, D.R., Michaelis, J., Otto, M., Just, S., Ludolph, A.C., Danzer, K.M., Freischmidt, A., Weishaupt, J.H., 2018. Dysregulation of a novel miR-1825/TBCB/TUBA4A pathway in sporadic and familial ALS. Cell. Mol. Life Sci. 75 (23), 4301–4319. https://doi.org/10.1007/s00018-018-2873-1.

Hersheson, J., Mencacci, N.E., Davis, M., MacDonald, N., Trabzuni, D., Ryten, M., Pittman, A., Paudel, R., Kara, E., Fawcett, K., Plagnol, V., Bhatia, K.P., Medlar, A.J., Stanescu, H.C., Hardy, J., Kleta, R., Wood, N.W., Houlden, H., 2013. Mutations in the autoregulatory domain of β-tubulin 4a cause hereditary dystonia. Ann. Neurol. 73, 546–553. https://doi.org/10.1002/ana.23832.

Jablonska, E., Vinceti, M., 2015. Selenium and human health: witnessing a copernican revolution? J. Environ. Sci. Health. C. Environ. Carcinog. Ecotoxicol. Rev. 33, 328–368. https://doi.org/10.1080/10590501.2015.1055163.

Janke, C., Kneussel, M., 2010. Tubulin post-translational modifications: encoding functions on the neuronal microtubule cytoskeleton. Trends Neurosci. 33, 362–372. https://doi.org/10.1016/j.tins.2010.05.001.

Kamelgarn, M., Chen, J., Kuang, L., Jin, H., Kasarskis, E.J., Zhu, H., 2018. ALS mutations of FUS suppress protein translation and disrupt the regulation of nonsense-mediated decay. Proc. Natl. Acad. Sci. U. S. A. 115, E11904–E11913. https://doi.org/10.1073/pnas.1810413115.

Kwiatkowski, T.J., Bosco, D.A., Leclerc, A.L., Tamrazian, E., Vanderburg, C.R., Russ, C., Davis, A., Gilchrist, J., Kasarskis, E.J., Munsat, T., Valdmanis, P., Rouleau, G.A., Hosler, B.A., Cortelli, P., de Jong, P.J., Yoshinaga, Y., Haines, J.L., Pericak-Vance, M.A., Yan, J., Ticozzi, N., Siddique, T., McKenna-Yasek, D., Sapp, P.C., Horvitz, H.R., Landers, J.E., Brown, R.H., 2009. Mutations in the FUS/TLS gene on chromosome 16 cause familial amyotrophic lateral sclerosis. Science 323, 1205–1208. https://doi.org/10.1126/science.1166066.

Landino, L.M., Koumas, M.T., Mason, C.E., Alston, J.A., 2007. Modification of tubulin cysteines by nitric oxide and nitroxyl donors alters tubulin polymerization activity †. Chem. Res. Toxicol. 20, 1693–1700. https://doi.org/10.1021/tx7001492.

Landino, L.M., Robinson, S.H., Skreslet, T.E., Cabral, D.M., 2004. Redox modulation of tau and microtubule-associated protein-2 by the glutathione/glutaredoxin reductase system. Biochem. Biophys. Res. Commun. 323, 112–117. https://doi.org/10.1016/j.bbrc.2004.08.065.

Livanos, P., Galatis, B., Apostolakos, P., 2014. The interplay between ROS and tubulin cytoskeleton in plants. Plant Signal. Behav. 9, e28069. https://doi.org/10.4161/psb.28069.

Lucarelli, E., Sangiorgi, L., Maini, V., Lattanzi, G., Marmiroli, S., Reggiani, M., Mordenti, M., Alessandra Gobbi, G., Scrimieri, F., Zambon Bertoja, A., Picci, P., 2002. Troglitazione affects survival of human osteosarcoma cells. Int. J. Cancer 98, 344–351.

Mackenzie, I.R., Nicholson, A.M., Sarkar, M., Messing, J., Purice, M.D., Pottier, C., Annu, K., Baker, M., Perkerson, R.B., Kurti, A., Matchett, B.J., Mittag, T., Temirov, J., Hsiung, G.-Y.R., Krieger, C., Murray, M.E., Kato, M., Fryer, J.D., Petrucelli, L., Zinman, L., Weintraub, S., Mesulam, M., Keith, J., Zivkovic, S.A., Hirsch-Reinshagen, V., Roos, R.P., Züchner, S., Graff-Radford, N.R., Petersen, R.C., Caselli, R.J., Wszolek, Z.K., Finger, E., Lippa, C., Lacomis, D., Stewart, H., Dickson, D.W., Kim, H.J., Rogaeva, E., Bigio, E., Boylan, K.B., Taylor, J.P., Rademakers, R., 2017. TIA1 mutations in amyotrophic lateral sclerosis and frontotemporal dementia promote phase separation and alter stress granule dynamics. Neuron 95, 808–816. https://doi.org/10.1016/j.neuron.2017.07.025. e9.

Magiera, M.M., Janke, C., 2014. Post-translational modifications of tubulin. Curr. Biol. 24, R351–R354. https://doi.org/10.1016/j.cub.2014.03.032.

Mandrioli, J., Michalke, B., Solovyev, N., Grill, P., Violi, F., Lunetta, C., Conte, A., Sansone, V.A., Sabatelli, M., Vinceti, M., 2017. Elevated levels of selenium species in cerebrospinal fluid of amyotrophic lateral sclerosis patients with disease-associated gene mutations. Neurodegener. Dis. 17, 171–180. https://doi.org/10.1159/000460253.

Maraldi, T., Guida, M., Zavatti, M., Resca, E., Bertoni, L., La Sala, G.B., De Pol, A., 2015. Nuclear Nox4 role in stemness power of human amniotic fluid stem cells. Oxid. Med. Cell. Longev. 2015, 1–11. https://doi.org/10.1155/2015/101304.

Maraldi, T., Riccio, M., Sena, P., Marzona, L., Nicoli, A., La Marca, A., Marmiroli, S., Bertacchini, J., La Sala, G., De Pol, A., 2009. MATER protein as substrate of PKCepsilon in human cumulus cells. Mol. Hum. Reprod. 15, 499–506. https://doi.org/10.1093/molehr/gap048.

Maraldi, T., Riccio, M., Zambonin, L., Vinceti, M., De Pol, A., Hakim, G., 2011. Low levels of selenium compounds are selectively toxic for a human neuron cell line through ROS/RNS increase and apoptotic process activation. Neurotoxicology 32, 180–187.

https://doi.org/10.1016/j.neuro.2010.10.008.
Millecamps, S., Julien, J.-P., 2013. Axonal transport deficits and neurodegenerative diseases. Nat. Rev. Neurosci. 14, 161–176. https://doi.org/10.1038/nrn3380.
Misra, S., Boylan, M., Selvam, A., Spallholz, J.E., Björnstedt, M., 2015. Redox-active selenium compounds–from toxicity and cell death to cancer treatment. Nutrients 7, 3536–3556. https://doi.org/10.3390/nu7053536.
Munnamalai, V., Suter, D.M., 2009. Reactive oxygen species regulate F-actin dynamics in neuronal growth cones and neurite outgrowth. J. Neurochem. 108, 644–661. https://doi.org/10.1111/j.1471-4159.2008.05787.x.
Naeem, A.S., Zhu, Y., Di, W.L., Marmiroli, S., O'Shaughnessy, R.F., 2015. AKT1-mediated Lamin A/C degradation is required for nuclear degradation and normal epidermal terminal differentiation. Cell Death Differ. 22 (12), 2123–2132. https://doi.org/10.1038/cdd.2015.62.
Penazzi, L., Bakota, L., Brandt, R., 2016. Microtubule dynamics in neuronal development, plasticity, and neurodegeneration. International Review of Cell and Molecular Biology. pp. 89–169. https://doi.org/10.1016/bs.ircmb.2015.09.004.
Pensato, V., Tiloca, C., Corrado, L., Bertolin, C., Sardone, V., Del Bo, R., Calini, D., Mandrioli, J., Lauria, G., Mazzini, L., Querin, G., Ceroni, M., Cantello, R., Corti, S., Castellotti, B., Soldà, G., Duga, S., Comi, G.P., Cereda, C., Sorarù, G., D'Alfonso, S., Taroni, F., Shaw, C.E., Landers, J.E., Ticozzi, N., Ratti, A., Gellera, C., Silani, V., S.L.A.G.E.N. Consortium, 2015. TUBA4A gene analysis in sporadic amyotrophic lateral sclerosis: identification of novel mutations. J. Neurol. 262, 1376–1378. https://doi.org/10.1007/s00415-015-7739-y.
Peters, O.M., Ghasemi, M., Brown, R.H., 2015. Emerging mechanisms of molecular pathology in ALS. J. Clin. Invest. 125, 1767–1779. https://doi.org/10.1172/JCI71601.
Resmini, G., Rizzo, S., Franchin, C., Zanin, R., Penzo, C., Pegoraro, S., Ciani, Y., Piazza, S., Arrigoni, G., Sgarra, R., Manfioletti, G., 2017. HMGA1 regulates the Plasminogen activation system in the secretome of breast cancer cells. Sci. Rep. 7, 11768. https://doi.org/10.1038/s41598-017-11409-4.
Rustici, G., Kolesnikov, N., Brandizi, M., Burdett, T., Dylag, M., Emam, I., Farne, A., Hastings, E., Ison, J., Keays, M., Kurbatova, N., Malone, J., Mani, R., Mupo, A., Pedro Pereira, R., Pilicheva, E., Rung, J., Sharma, A., Tang, Y.A., Ternent, T., Tikhonov, A., Welter, D., Williams, E., Brazma, A., Parkinson, H., Sarkans, U., 2012. ArrayExpress update—trends in database growth and links to data analysis tools. Nucleic Acids Res. 41, D987–D990. https://doi.org/10.1093/nar/gks1174.
Smith, B.N., Ticozzi, N., Fallini, C., Gkazi, A.S., Topp, S., Kenna, K.P., Scotter, E.L., Kost, J., Keagle, P., Miller, J.W., Calini, D., Vance, C., Danielson, E.W., Troakes, C., Tiloca, C., Al-Sarraj, S., Lewis, E.A., King, A., Colombrita, C., Pensato, V., Castellotti, B., de Belleroche, J., Baas, F., ten Asbroek, A.L., Sapp, P.C., McKenna-Yasek, D., McLaughlin, R.L., Polak, M., Asress, S., Esteban-Pérez, J., Muñoz-Blanco, J.L., Simpson, M., van Rheenen, W., Diekstra, F.P., Lauria, G., Duga, S., Corti, S., Cereda, C., Corrado, L., Sorarù, G., Morrison, K.E., Williams, K.L., Nicholson, G.A., Blair, I.P., Dion, P.A., Leblond, C.S., Rouleau, G.A., Hardiman, O., Veldink, J.H., van den Berg, L.H., Al-Chalabi, A., Pall, H., Shaw, P.J., Turner, M.R., Talbot, K., Taroni, F., García-Redondo, A., Wu, Z., Glass, J.D., Gellera, C., Ratti, A., Brown, R.H., Silani, V., Shaw, C.E., Landers, J.E., D'Alfonso, S., Mazzini, L., Comi, G.P., Del Bo, R., Ceroni, M., Gagliardi, S., Querin, G., Bertolin, C., 2014. Exome-wide rare variant analysis identifies TUBA4A mutations associated with familial ALS. Neuron 84, 324–331. https://doi.org/10.1016/j.neuron.2014.09.027.
Sun, R., Eriksson, S., Wang, L., 2012. Oxidative stress induced *S* -glutathionylation and proteolytic degradation of mitochondrial thymidine kinase 2. J. Biol. Chem. 287, 24304–24312. https://doi.org/10.1074/jbc.M112.381996.
Tischfield, M.A., Cederquist, G.Y., Gupta, M.L., Engle, E.C., 2011. Phenotypic spectrum of the tubulin-related disorders and functional implications of disease-causing mutations. Curr. Opin. Genet. Dev. 21, 286–294. https://doi.org/10.1016/j.gde.2011.01.003.
Tyanova, S., Temu, T., Cox, J., 2016. The MaxQuant computational platform for mass spectrometry-based shotgun proteomics. Nat. Protoc. 11, 2301–2319. https://doi.org/10.1038/nprot.2016.136.
Vinceti, M., Filippini, T., Wise, L.A., 2018a. Environmental selenium and human health: an update. Curr. Environ. Heal. Reports 5, 464–485. https://doi.org/10.1007/s40572-018-0213-0.
Vinceti, M., Mandrioli, J., Borella, P., Michalke, B., Tsatsakis, A., Finkelstein, Y., 2014. Selenium neurotoxicity in humans: bridging laboratory and epidemiologic studies. Toxicol. Lett. 230, 295–303. https://doi.org/10.1016/j.toxlet.2013.11.016.
Vinceti, M., Solovyev, N., Mandrioli, J., Crespi, C.M., Bonvicini, F., Arcolin, E., Georgoulopoulou, E., Michalke, B., 2013. Cerebrospinal fluid of newly diagnosed amyotrophic lateral sclerosis patients exhibits abnormal levels of selenium species including elevated selenite. Neurotoxicology 38, 25–32. https://doi.org/10.1016/j.neuro.2013.05.016.
Vinceti, M., Vicentini, M., Wise, L.A., Sacchettini, C., Malagoli, C., Ballotari, P., Filippini, T., Malavolti, M., Rossi, P.G., 2018b. Cancer incidence following long-term consumption of drinking water with high inorganic selenium content. Sci. Total Environ. 635, 390–396. https://doi.org/10.1016/j.scitotenv.2018.04.097.
Wilson, C., González-Billault, C., 2015. Regulation of cytoskeletal dynamics by redox signaling and oxidative stress: implications for neuronal development and trafficking. Front. Cell. Neurosci. 9, 381. https://doi.org/10.3389/fncel.2015.00381.
Wolozin, B., 2014. Physiological protein aggregation run amuck: stress granules and the genesis of neurodegenerative disease. Discov. Med. 17, 47–52.
Yang, L., Zhang, J., Kamelgarn, M., Niu, C., Gal, J., Gong, W., Zhu, H., 2015. Subcellular localization and RNAs determine FUS architecture in different cellular compartments. Hum. Mol. Genet. 24, 5174–5183. https://doi.org/10.1093/hmg/ddv239.